The effect of thickness of Nylon 6,6 nanofibrous mat on Modes I-II fracture mechanics of UD and woven composite laminates

T. Brugo[a], R. Palazzetti[b,*]

[a] *University of Bologna, Department of Industrial Engineering, viale del Risorgimento 2, 40136 Bologna, Italy*
[b] *University of Strathclyde, DMEM department, 75 Montrose Street, G1 1XJ, Glasgow, UK*

Abstract

This paper presents an experimental investigation on epoxy resin-carbon fibers composites interleaved with Nylon 6,6 nanofibers. In particular, the paper focuses on the effect of the thickness of the nanoreinforce into two types of laminae: unidirectional (UD) and plain wave (PW). The effectiveness of the nanoreinforce has been addressed by comparing critical and propagation energy release rates, calculated by testing samples under Mode I and Mode II fracture mechanic loads.
Experiments show a general improvement in delamination resistance when the nanofibers are interleaved. Nevertheless slightly different behaviour has been found between the two types of lamina: micrographs of crack paths have been used to explain the reinforce mechanisms and such differences, suggesting a strong interaction between the nature of the fabric and the thickness of the nanointerlayer.

Keywords: Delamination, Composite Materials, Fracture Mechanics, Nanofibers

*Principal corresponding author
Email addresses: tommasomaria.brugo@unibo.it (T. Brugo), roberto.palazzetti@strath.ac.uk (R. Palazzetti)

1. Introduction

Interleaving composite laminates with polymeric nanofibers is now an established method to reduce the risk of delamination without affecting the in-plane properties of the original laminate [1]. The authors have already deeply investigated mechanical properties of carbon fiber reinforced plastic (CFRP) interleaved with Nylon 6,6 nanofibers produced by electrospinning [2–6], showing very positive results.

Plenty of research has been done on the topic of composites interleaved with nanofibers, and there is a general agreement that under certain conditions of resin-polymer compatibility, size and amount of interleave, and type of material, nanofibers can bring significant benefits to the composite [7–11].

This paper presents an experimental campaign on samples made of unidirectional (UD) and Plain Weave (PW) laminae, aiming (*i*) to investigate the effect of the thickness of the nanoreinforce, and (*ii*) to study the different behaviours of the two types of laminae when interleaved with nanofibers. Specimens have been tested under double cantilever beam (DCB) and end notched flexure (ENF) load modes. The energy release rates at initiation (G_C) and propagation (G_R) of the crack have been determined for each configuration to assess the effect of the nanointerleave.

Molnar et al. [12] Charpy-impacted UD and PW specimens, showing 11% and 7% improvement respectively in interlaminar shear strength when nanofibers are employed. Bilge et al. [13] used P(St-co-GMA) copolymer to produce nanofibers to interleave $(0)_6$ and $(0/90)_{6,woven}$ laminates, which have been uni-axial tested. They showed that the ultimate tensile strength increased 12% and 18% in UD and PW laminates respectively. Fracture mechanics is of primary importance for the study of the delamination behaviour of materials, and the only work comparing fracture mechanics behaviour of UD and PW nanomodified samples is that of Daelemans et al. [14]. They tested virgin and nanomodified samples under Mode I and Mode II loading condition, using two different density of PA6,6 and PA6,9 nanofibrous veils. Their results showed that nanofibre-interleaved specimens had large improvement of $G_{II,C}$ both for UD and PW laminates. Poorer results have been found on Mode I crack propagation, due to a less optimal loading of the nanofibres, dependent on the primary reinforcement fabric architecture, and the presence of a carbon fibre bridging zone. Their results, supported by Scanning Electron Microscopy (SEM) pictures of the fractured surfaces, highlight the importance of nanofiber bridging in arresting the crack propa-

gation.
In this paper a different outcome has been found, as well as a different reinforcing mechanism; micrographs of the crack path taken on the tested specimens will be used to explain the results.
Liu et al. [15, 16] nanoreinforced laminates with epoxy 609 polymer, and tested samples under Mode I and Mode II loads with different thickness of the nanoreinforce. They found that 70 and 128.1 μm are the optimal nanoreinforce thickness for Mode I and Mode II loads respectively: values lower or above those cause the interlaminar fracture toughness to drop down. Zhang et al. [17] investigated the effect of polyetherketone cardo (PEK-C) nanofibre interlayer thickness onto carbon/epoxy composites, showing that increasing nanofibre interlayer thickness improves the fracture toughness but compromises the flexure performance. Zhang et al. [18] used dissolvable thermoplastic interleaves and electrospun fibers. They tested 4 different nanofibrous thicknesses showing a constant trend of improved energy release rates at both initiation and propagation stages.
This present paper shows a general improvement of energy release rates when a nanolayer is interleaved, with significantly better results for woven laminates.
Micrographs of the crack paths have been used to explain the said differences and to illustrate the reinforcing mechanism.

2. Materials and methods

2.1. Sample preparation

UD samples have been prepared stacking 20 plies of 130 g/m^2 unidirectional carbon/epoxy prepreg (HS15/130DLN2-IMP505L) supplied by Impregnatex Composite Srl (Milan, Italy).
PW samples have been prepared stacking 14 plies of 220 g/m^2 plain weave prepreg (GG204P-IMP503Z), supplied by Impregnatex Composite Srl (Milan, Italy)
Nylon 6,6 Zytel E53NC010 provided by DuPont was used for producing nanofibers by means of electrospinning using the process parameters showed in [19]. The polymer solution was made dissolving 20% of Nylon 6,6 in a 70:30 mixture of TFA and Formic Acid. Nanofibers of 350-400 nm diameter were randomly distributed in 40 and 90 μm thick mats. Nanofibers were kept in oven at 40^oC overnight to remove residual solvents and moisture before being integrated into the laminate.

Before the curing process, all samples were put under vacuum (850 $mbar$) for 24 hours to ensure the perfect penetration of the matrix into the nanofibrous mat. Then all samples where cured following the curing cycle described in [20]
Nanomodified specimens were interleaved in the mid-plane with the nanofibrous mat as presented in [20]. A 30 μm thick PTFE film was also inserted in the mid-interface of all the specimens during the lay-up to create an initial artificial crack.
From here on in virgin samples will be identified with the character "V", and nanomodified ones with the characters "NY".
In total 6 different configurations have been manufactured as summarised in Table 1.

Code	**Nanofibers**	**Mat thickness**	**Fabric**
V_{UD}	no	-	UD
V_{PW}	no	-	PW
$NY_{40,UD}$	yes	$40\mu m$	UD
$NY_{90,UD}$	yes	$90\mu m$	UD
$NY_{40,PW}$	yes	$40\mu m$	PW
$NY_{90,PW}$	yes	$90\mu m$	PW

Table 1: Summary of the tested configurations

For each configuration a rectangular panel was fabricated, and 6 samples were extracted from each one: half of them where tested under mode I, the other half under Mode II. No appreciable differences in thickness between V and NY samples have been registered.

2.2. Fracture Mechanics Tests

2.2.1. Mode I tests

DCB samples have been prepared according to the ASTM D5528 [21]: 140 mm long, 20 mm wide, initial crack of 45 mm, aluminium blocks glued on the tip for the application of the load.
DCB tests have been performed in order to calculate the energy release rate for mode I loading G_I, using Eq. 1, from the Modified Beam Theory (MBT) presented in [21]:

$$G_I = \frac{3F\delta}{2Ba} \tag{1}$$

where F, δ, B and a are the force, the displacement of the load head, the specimen width and the crack length respectively.
The tests were carried out in a servo-hydraulic press machine (Instron 8033) equipped with a dedicated in-house designed and manufactured 250 N load cell, under displacement control condition, at a constant crosshead speed of 3 mm/min. A uniball-like feature on the grippers avoided any undesired loads. During each test, the load-displacement curve was recorded and the crack propagation was visually determined by means of a high-resolution camera focusing on the edge of the specimen.
For a better understanding of the results, the crack propagation is split into two stages: the initiation stage, in which the delamination onset starts from the artificial crack (critical energy release rate, $G_{I,C}$) and the propagation stage evaluating the crack between 60 and 80 mm of length (propagation energy release rate, $G_{I,R}$).

2.2.2. Mode II tests

No official international standard for ENF tests has been developed so far, therefore the authors followed the guidelines provided in [22], and manufactured specimens 130 mm long, 20 mm wide, with an initial crack of 28 mm. The span between the two supports was 80 mm.
From the ENF tests the levels of critical and propagation fracture toughness, $G_{II,C}$ and $G_{II,R}$ respectively, have been determined for each specimen using Eq. 2 [22]:

$$G_{II} = \frac{9F\delta a^2}{2B\left(0.25L^3 + 3a^3\right)} \tag{2}$$

where L is the span width.
The tests were carried out in a servo-hydraulic press machine (Instron 8033) equipped with a 2 kN load cell, under displacement control condition, at a constant crosshead speed of 1 mm/min. During each test, the load-displacement curve was recorded and the crack propagation was visually determined by means of a high-resolution camera focusing on the edge of the specimens.

3. Results and discussion

The next section presents separately the results of the two types of test, highlighting the different effect of the nanofiber interleaving the two different types of prepreg.

3.1. DCB

Figure 1 shows the force-displacement curves of the representative sample of each configuration.

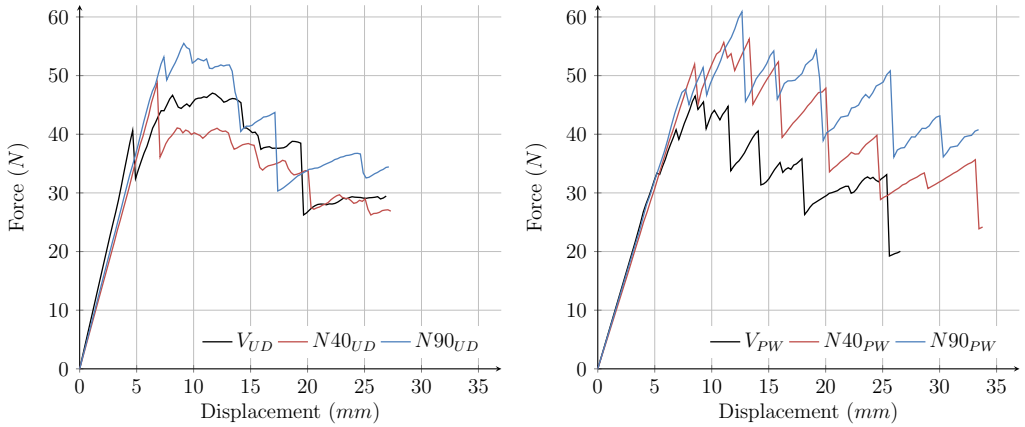

(a) UD specimens (b) Woven specimens

Figure 1: Representative DCB force-displacement curves

The maximum force registered during the tests has been extracted from the charts and presented in Table 2.

The presence of the nanofiber postpones the crack initiation and increases the maximum force value on both UD and PW laminates.
As mentioned above, G_I has been calculated several times during the tests, and the resulting R-curves, showing the energy release rates $G_{I,C}$ and $G_{I,R}$ as function of the crack length, are plotted in Figure 2.

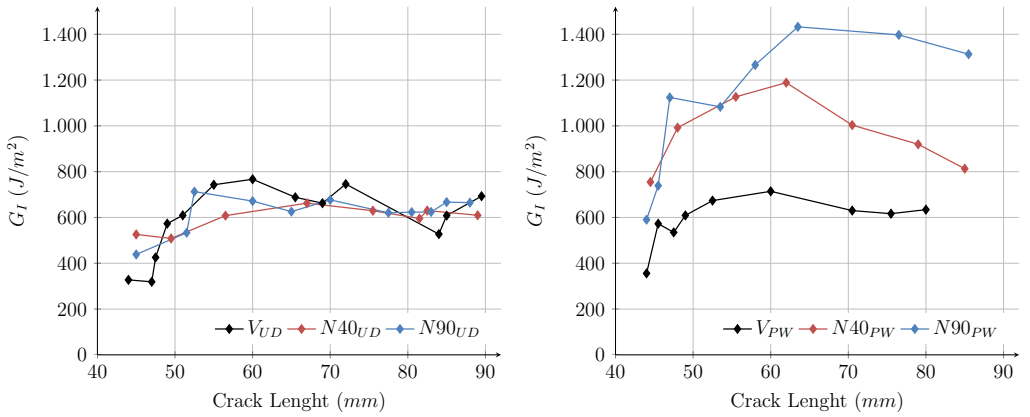

(a) UD specimens (b) Woven specimens

Figure 2: Representative R-Curves for DCB tests

It can be observed that for all the specimens the values of G_I are minimum at the beginning of the crack propagation and then increase significantly up to the stable value.
$G_{I,C}$ and $G_{I,R}$ have been determined and presented in Figure 3 and Table 2.

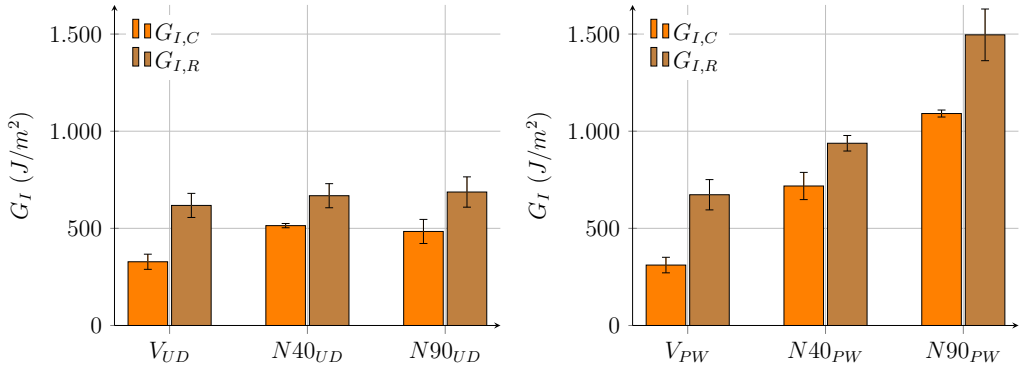

(a) UD specimens (b) Woven specimens

Figure 3: Initiation and propagation energy release rate for Mode I loading.

Results show a general improvement on both UD and PW samples when the nanofibers are employed. Nevertheless, two different effects can be observed:

- from the R-curves in Figure 2, the fracture toughness increases due to the presence of the nanofiber for woven laminates is registered at

	F_{max} (N)		$G_{I,C}$ (J/m^2)		$G_{I,R}$ (J/m^2)	
			UD			
	Mean	Δ (%)	Mean	Δ (%)	Mean	Δ (%)
V	45.12±1.77	-	328±39	-	618±62	-
NY_{40}	49.47±2.52	+10±7	514±11	$+56 \pm 12$	668±62	$+8 \pm 14$
NY_{90}	51.5±3.88	+14±10	484±62	$+48 \pm 23$	687±78	$+11 \pm 16$
			PW			
	Mean	Δ (%)	Mean	Δ (%)	Mean	Δ (%)
V	46.63±1.43	-	311±40	-	673±78	-
NY_{40}	55.37±2.93	+19±7	718±70	$+131 \pm 31$	938±40	$+40 \pm 14$
NY_{90}	62.47±1.69	+34±5	1091±18	$+250 \pm 35$	1496±133	$+122 \pm 27$

Table 2: Results of DCB tests

both initiation and propagation stages. On the other hand, the fracture toughness increment for UD laminates is only regustered at the initiation, while inprovement at propagation are negligible;

- the bar graphs in Figure 3 show that fracture toughness increases in PW laminates whit the nanofiber mat thickness, while UD laminates are not affected by the nanoreinforce thickness.

The reason for this phenomena will be clarified by the micrograph analysis shown in §3.3.

3.2. ENF

Figure 4 shows the force-displacement curves of the representative samples of each configuration, extracted during ENF tests.

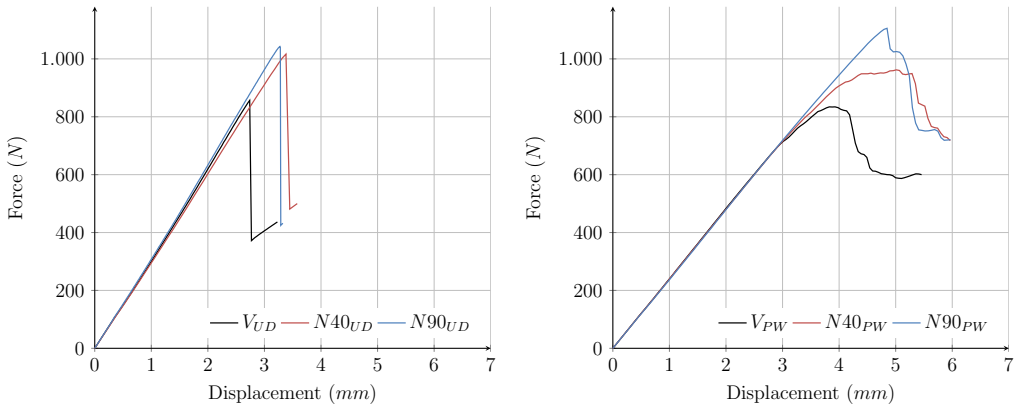

(a) UD specimens (b) Woven specimens

Figure 4: Representative ENF force-displacement curves

The force vs. displacement curves for UD laminates show an abrupt drop of the load associated to a sudden non-stable crack propagation, making the rest of the test useless for the purposes of this paper; on the other hand, in woven laminates the crack propagates stably with a stick-slip behaviour. The maximum force registered during the tests has been extracted from the charts and presented in Table 3.

As mentioned above, G_{II} has been calculated several times during the tests, and the results are plotted in Figure 5.

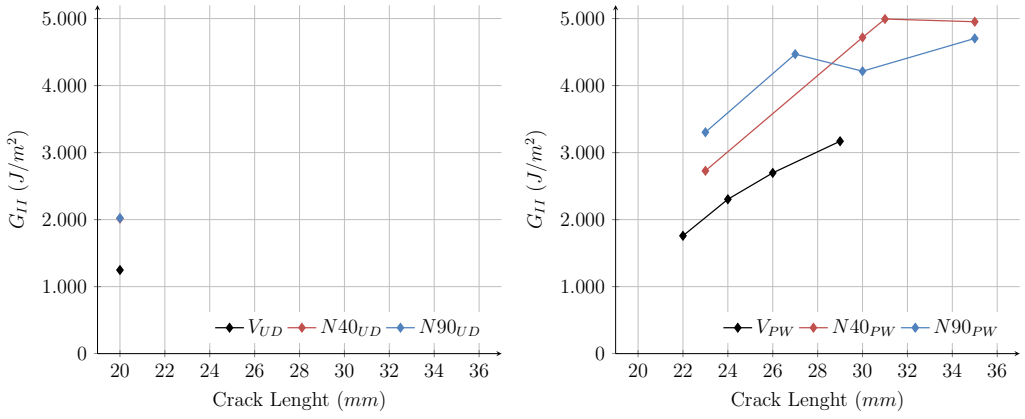

(a) UD specimens (b) Woven specimens

Figure 5: Representative R-Curves for ENF tests

For the reason explained above, experiments on UD samples allowed to measure fracture toughness only at the initiation stage; tests carried out on PW samples instead have been also completed for propagation stage.
Critical and propagation energy release rates are plotted in the charts of Figure 6.

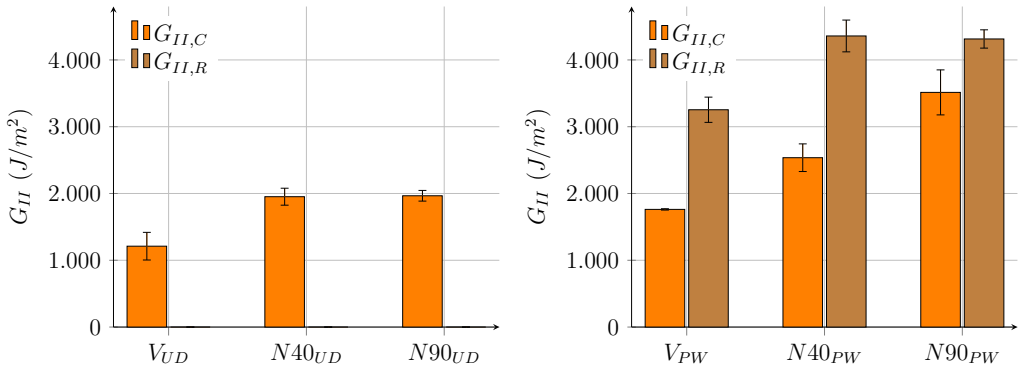

(a) UD specimens (b) Woven specimens

Figure 6: Initiation and propagation energy release rate for Mode II loading

Table 3 summarises the increments of G_{II} due to the nanofiber interleaving.

	F_{max} (N)		$G_{II,C}$ (J/m^2)		$G_{II,R}$ (J/m^2)	
			UD			
	Mean	Δ (%)	Mean	Δ (%)	Mean	Δ (%)
V	859±54	-	1211±207	-	N/D	-
NY_{40}	962±62	+12±10	1952±127	+61 ± 20	N/D	-
NY_{90}	1045±2	+22±6	1966±80	+62 ± 19	N/D	-
			PW			
	Mean	Δ (%)	Mean	Δ (%)	Mean	Δ (%)
V	849±13	-	1762±10	-	3254±189	-
NY_{40}	944±22	+11±4	2536±207	+44 ± 12	3514± 337	+34 ± 10
NY_{90}	1060±42	+25±5	4359±238	+99 ± 19	4314±137	+32 ± 7

Table 3: Results of ENF tests

Results show a general improvement on both UD and PW samples when the nanofibers are employed. Similarly to what shown for Mode I, at the

initiation stage, fracture toughness of UD laminates is not influenced by the nanofiber mat thickness, while PW laminates show growing rates of performance with the increase of the mat thickness. Different results can be seen at propagation stage, where PW $G_{II,R}$ is not affected by the nanomat thickness. Overall, higher increments are registered for Mode I than Mode II.

3.3. Micrography

The results illustrated in the previous sections can be explained with micrographs. By means of an optical microscope, images of crack paths have been captured to investigate the nanofiber's reinforce mechanism
Photographs in Figure 7 show the crack paths of DCB PW V, NY_{40} and NY_{90} samples. Green lines indicate the nanolayer.

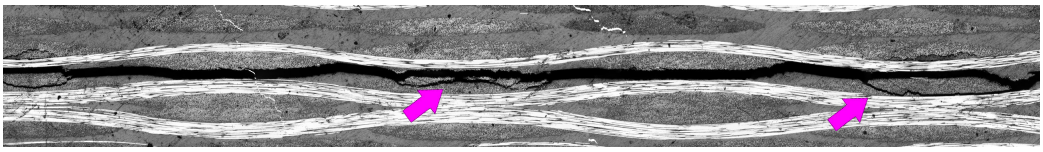

(a) Crack path in a DCB PW V specimen

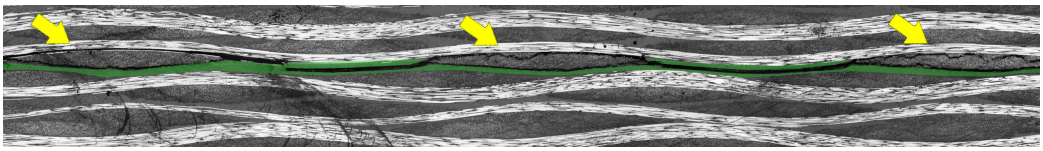

(b) Crack path in a DCB PW NY_{40} specimen

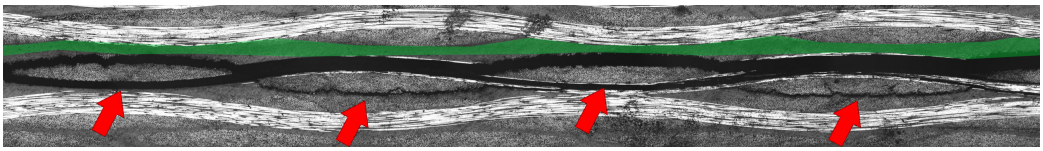

(c) Crack path in a DCB PW NY_{90} specimen

Figure 7: V and NY crack paths from DCB PW samples.

The above images give an indication of of the nano reinforcement mechanism. Figure 7a shows the crack following a linear path, with very small deviations from an ideal straight line, and a few small extra fractures on the adjacent layers, as indicated by the purple arrows. Nanomodified samples,

shown in Figures 7b and 7c, instead, show a different behaviour: while propagating, the crack deviates from the toughened, nanoreinforced interface, and is forced to follow a longer, zig-zag shaped path, as pointed by yellow and red arrows. It will cause to break not only a larger amount of matrix, but also some of the carbon fibers belonging to the adjacent layers, thus requiring higher energy to propagate in comparison with pristine specimens.
Furthermore, comparing Figure 7b with Figure 7c, it can be noted that the thicker nanofibrous mat covers almost the entire interlayer, filling also those areas that due to the woven nature of the fabric, present higher matrix content (the so-called resin pockets). The same can not be said for the thinner interlayesr, which only partially cover the interface. Thicker nanolayer can effectively link the two plies it is inserted between along the entire interface. Therefore, crack propagation in PW NY_{90} specimens is constantly hindered by the nanointerlaye and forced to bifurcate and propagate through the carbon tow of adjacent layers.

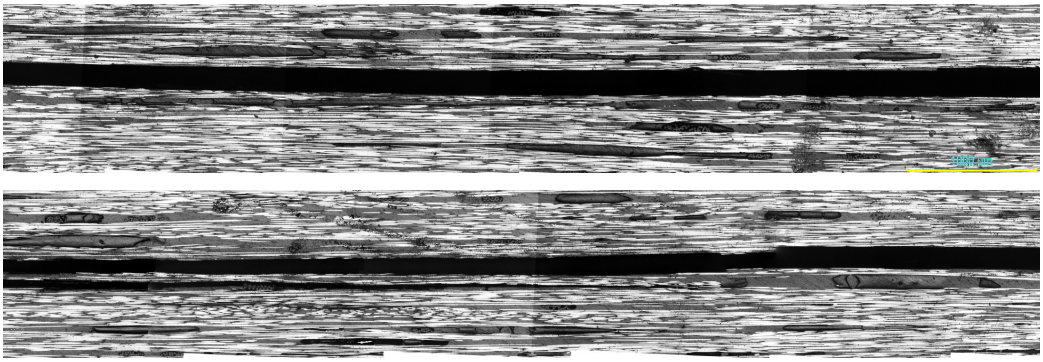

(a) Crack path in a DCB UD specimen

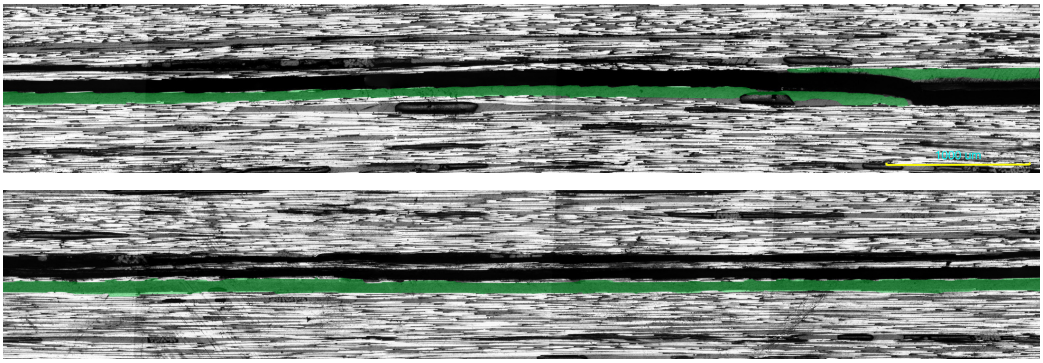

(b) Crack path in a DCB UD NY_{90} specimen

Figure 8: Crack paths of DCB V and NY_{90} samples. Crack starts top-right

Photographs in Figure 8, top to bottom, right to left, shows the crack paths of DCB virgin and nanomodified UD samples, and two main things can be observed:

- the crack, induced by the Teflon layer, tents to propagate through the nanointerlayer (Figure 8b), which makes the reinforce to play an active role in hindering the crack initiation and increasing the fracture toughness at the onset. On the other hand, during the propagation stage, the crack deviates from the toughened region to the adjacent, not reinforced interlayer, propagating along the direction of the carbon fibres. The same would happen for PW laminates (see Figure 7b and Figure 7c) if it was not for the more complex texture of the woven fabric, which stops the propagation of the crack inside the carbon layer,

and forces it to stay in the nano-modified interlayer. This explains the ineffectiveness of the nanofibers on crack propagation inside UD laminates and their opposite effect on woven fabric;

- the different influence of the nano-mat thickness on the fracture toughness of UD and PW laminates can be explained comparing the two cross sections in Figure 7c and Figure 8b: UD laminates, having all the carbon fibres aligned along one direction, create a flat thin interlayer, while the woven nature of PW laminates creates a wavy thick interlayer. It is therefore necessary a thicker nanoreifnroce to cover all the interface to make it effective against crack propagation.

4. Conclusion

This paper presented an experimental study on the effect of the thickness of a nanofibrous interlayer into plain wave and unidirectional epoxy-based composite laminates.
The results showed a significant improvement when nanofibers are employed under both DCB and ENF loading conditions for both the UD and PW configurations of laminate.
In general better results have been found for PW samples, for DCB loads, and for thicker nanoreinforce.
The increased critical energy release rates $G_{I,C}$ and $G_{II,C}$, proved that the presence of nanofibers hinder the crack initiation by reinforcing the matrix. Furthermore, micrographs showed that during the propagation stage, the crack in nanomodified samples is forced to break a larger amount of matrix compared to virgin samples, requiring higher energy to propagate, and that this energy increases with the thickness of the nanoreinforce.
UD samples are less affected by nanofibers due to the fact that the crack tends to cross plies and not to propagate in the same interface the nanolayer is laid.
Eventually the micrographs explained the mechanical results, suggesting a strong interaction betwenn the nature of the fabric and the thickness on the nanoreinforce. In general the nanoreinforce increases the fracture toughness at the initiation for all the configurations, while the propagation stage is significantly dependent on the amount of the reinforce and on the nature of the fabric.

Acknowledgement

The Authors would like to thank Professors Andrea Zucchelli and Giangiacomo Minak from University of Bologna, and owe them a considerable debt of gratitude for their invaluable help and generosity of both time and spirit, throughout the many fruitful and illuminating discussions we had during the whole development of the work.

References

[1] K. Shivakumar, R. Panduranga, Interleaved polymer matrix composites - A review, Collection of Technical Papers - AIAA/ASME/ASCE/AHS/ASC Structures, Structural Dynamics and Materials Conference (2013) 1–13doi:10.2514/6.2013-1903.
URL http://www.scopus.com/inward/record.url?eid=2-s2.0-84881364474{&}partnerID=tZOtx3y1

[2] R. Palazzetti, Flexural behavior of carbon and glass fiber composite laminates reinforced with Nylon 6,6 electrospun nanofibers, Journal of Composite Materials 49 (27) (2015) 3407–3413. doi:10.1177/0021998314565410.
URL http://jcm.sagepub.com/cgi/doi/10.1177/0021998314565410

[3] H. Saghafi, R. Palazzetti, A. Zucchelli, G. Minak, Influence of electrospun nanofibers on the interlaminar properties of unidirectional epoxy resin/glass fiber composite laminates, Journal of Reinforced Plastics and Composites 34 (11) (2015) 907–914.

[4] S. Alessi, M. di Filippo, C. Dispenza, M. Focarete, C. Gualandi, R. Palazzetti, G. Pitarresi, A. Zucchelli, Effects of Nylon 6,6 Nanofibrous Mats on Thermal Properties and Delamination Behavior of High Performance CFRP Laminates, Polymer Composites 36 (7) (2015) 1303–1313. doi:10.1002/pc.

[5] F. Moroni, R. Palazzetti, A. Zucchelli, A. Pirondi, A numerical investigation on the interlaminar strength of nanomodified composite interfaces, Composites Part B: Engineering 55 (2013) 635–641. doi:10.1016/j.compositesb.2013.07.004.

URL http://linkinghub.elsevier.com/retrieve/pii/S1359836813003739

[6] H. Saghafi, R. Palazzetti, A. Zucchelli, G. Minak, Impact response of glass/epoxy laminate interleaved with nanofibrous mats, Engineering Solid Mechanics 1 (2013) 85–90. doi:10.5267/j.esm.2013.09.002.

[7] K. Shivakumar, S. Lingaiah, H. Chen, P. Akangah, G. Swaminathan, L. Russell, Polymer Nanofabric Interleaved Composite Laminates, AIAA Journal 47 (7) (2009) 1723–1729. doi:10.2514/1.41791.
URL http://arc.aiaa.org/doi/abs/10.2514/1.41791

[8] X. Wu, A. L. Yarin, Recent progress in interfacial toughening and damage self-healing of polymer composites based on electrospun and solution-blown nanofibers: An overview, Journal of Applied Polymer Science 130 (4) (2013) 2225–2237. doi:10.1002/app.39282.

[9] B. De Schoenmaker, S. Van Der Heijden, I. De Baere, W. Van Paepegem, K. De Clerck, Effect of electrospun polyamide 6 nanofibres on the mechanical properties of a glass fibre/epoxy composite, Polymer Testing 32 (8) (2013) 1495–1501. doi:10.1016/j.polymertesting.2013.09.015.

[10] V. Koissin, L. L. Warnet, R. Akkerman, Delamination in carbon-fibre composites improved with in situ grown nanofibres, Engineering Fracture Mechanics 101 (2013) 140–148. doi:10.1016/j.engfracmech.2012.09.006.
URL http://dx.doi.org/10.1016/j.engfracmech.2012.09.006

[11] L. Daelemans, S. van der Heijden, I. De Baere, H. Rahier, W. Van Paepegem, K. De Clerck, Using aligned nanofibres for identifying the toughening micromechanisms in nanofibre interleaved laminates, Composites Science and Technology 124 (2016) 17–26. doi:10.1016/j.compscitech.2015.11.021.

[12] K. Molnar, E. Kostakova, L. Meszaros, The effect of needleless electrospun nanofibrous interleaves on mechanical properties of carbon fabrics/epoxy laminates, Express Polymer Letters 8 (1) (2013) 62–72. doi:10.3144/expresspolymlett.2014.8.

URL http://www.expresspolymlett.com/letolt.php?file=EPL-0004628{&}mi=c

[13] K. Bilge, S. Venkataraman, Y. Menceloglu, M. Papila, Global and local nanofibrous interlayer toughened composites for higher in-plane strength, Composites Part A: Applied Science and Manufacturing 58 (2014) 73–76. doi:10.1016/j.compositesa.2013.12.001.
URL http://linkinghub.elsevier.com/retrieve/pii/S1359835X13003291

[14] L. Daelemans, S. van der Heijden, I. De Baere, H. Rahier, W. Van Paepegem, K. De Clerck, Nanofibre bridging as a toughening mechanism in carbon/epoxy composite laminates interleaved with electrospun polyamide nanofibrous veils, Composites Science and Technology 117 (2015) 244–256. doi:10.1016/j.compscitech.2015.06.021.
URL http://dx.doi.org/10.1016/j.compscitech.2015.06.021

[15] L. Liu, Y. Liang, G. Xu, H. Zhang, Z. Huang, Mode I Interlaminar Fracture of Composite Laminates Incorporating with Ultrathin Fibrous Sheets, Journal of Reinforced Plastics and Composites 27 (11) (2008) 1147–1162. doi:10.1177/0731684407086504.

[16] L. Liu, Z. Huang, G. Xu, Y. Liang, G. Dong, Mode II Interlaminar Delamination of Composite Laminates Incorporating With Polymer Ultrathin Fibers, Polymer Composites 03. doi:10.1002/pc.

[17] J. Zhang, T. Lin, X. Wang, Electrospun nanofibre toughened carbon/epoxy composites: Effects of polyetherketone cardo (PEK-C) nanofibre diameter and interlayer thickness, Composites Science and Technology 70 (11) (2010) 1660–1666. doi:10.1016/j.compscitech.2010.06.019.
URL http://dx.doi.org/10.1016/j.compscitech.2010.06.019http://linkinghub.elsevier.com/retrieve/pii/S0266353810002575

[18] H. Zhang, A. Bharti, Z. Li, S. Du, E. Bilotti, T. Peijs, Localized toughening of carbon / epoxy laminates using dissolvable thermoplastic interleaves and electrospun fibres, Composites Part A 79 (2015) 116–126. doi:10.1016/j.compositesa.2015.09.024.
URL http://dx.doi.org/10.1016/j.compositesa.2015.09.024

[19] H. Saghafi, A. Zucchelli, R. Palazzetti, G. Minak, The effect of interleaved composite nanofibrous mats on delamination behavior of polymeric composite materials, Composite Structures 109 (2014) 41–47. doi:10.1016/j.compstruct.2013.10.039.
URL http://linkinghub.elsevier.com/retrieve/pii/S0263822313005527

[20] T. Brugo, G. Minak, A. Zucchelli, H. Saghafi, M. Fotouhi, An Investigation on the Fatigue based Delamination of Woven Carbon-epoxy Composite Laminates Reinforced with Polyamide Nanofibers, Procedia Engineering 109 (2015) 65–72. doi:10.1016/j.proeng.2015.06.208.
URL http://linkinghub.elsevier.com/retrieve/pii/S1877705815011704

[21] ASTM D5528, Standard test method for Mode I interlaminar fracture toughness of unidirectional fiber-reinforced polymer matrix composites, Annual Book of ASTM Standards.

[22] European Structural Integrity Society; 1993., Protocol No 2 for interlaminar fracture toughness testing of composites: Mode II, Bordeaux, 1993.